Thermal dileptons from π-ρ interactions in a hot pion gas

R. Baier and M. Dirks
Fakultät für Physik, Universität Bielefeld, D-33501 Bielefeld, Germany

K. Redlich
Institute for Theoretical Physics, University of Wroclaw, PL-50204 Wroclaw, Poland
and GSI, PF 110552, D-64220 Darmstadt, Germany
(Received 2 October 1996)

The production of low mass dileptons from π-ρ interactions in a hot medium is studied. Applying finite temperature perturbation theory the dilepton rate is computed up to order g_ρ^2. For dilepton masses below the ρ the two-body reactions $\pi\pi\rightarrow\rho\gamma^*$, $\pi\rho\rightarrow\pi\gamma^*$, and the decay process $\rho\rightarrow\pi\pi\gamma^*$ give significant contributions. Nonequilibrium contributions to the thermal rate are estimated, including the modification of the particle distribution function with a nonzero pion chemical potential. A comparison of the dilepton rate with the recent data measured in nucleus-nucleus collisions at CERN SPS energy by the CERES Collaboration is also performed. It is shown that the additional thermal dileptons from π-ρ interactions can partially account for the excess of the soft dilepton yield seen experimentally. [S0556-2821(97)03107-X]

PACS number(s): 13.85.Qk, 11.10.Wx, 12.38.Bx, 25.75.Dw

I. INTRODUCTION

Dilepton production is one of the interesting tools to study collective effects in strongly interacting matter produced in ultrarelativistic heavy ion collisions [1–4]. This is particularly evident from the recent CERN experimental data at Super Proton Synchrotron (SPS) collision energy. A significant enhancement of the dilepton spectrum measured in A-A collisions as compared with p-p and p-A collisions is reported. Two experiments, CERES/NA45 [5] and HELIOS/3 [6], have measured dileptons in the low mass range in S-Au, Pb-Au, and S-W collisions, respectively. Both these experiments have reported an excess of dileptons with invariant masses between 0.25 and 1 GeV in A-A nuclear collisions, compared to expected [5] or measured [6] spectra in p-A collisions.

These remarkable results indicate the appearance of collective phenomena in heavy ion collisions, such as thermalization of the medium after the collision. Since the temperatures are not yet to be expected as high, in particular, the reactions involving pions and ρ mesons are important and have to be considered. In the kinematical window of low mass dileptons pion annihilation with the ρ in the intermediate state is a basic source of thermal dileptons, also responsible for the low mass dilepton enhancement reported by the CERN experiments. Indeed, recent theoretical calculations show that close to the ρ peak the thermal production rate due to pion annihilation is compatible with the experimental data [7,8]. However, neither the size of the excess below the ρ peak nor the shape of the distribution is quantitatively explained by this contribution alone. In a thermal medium, however, the partial restoration of chiral symmetry in hot and dense hadronic matter may modify the properties of vector mesons, especially their mass or decay width [9,10]: In Ref. [7] it is shown that thermal dilepton production due to the pion annihilation process together with the assumption of a decreasing ρ meson mass leads to a quantitative explanation of the enhancement of the low mass dileptons observed by the CERES and by the HELIOS/3 experiments.

The above results together with previous theoretical studies [11–13] suggest the importance of pion scattering in a medium as a source of soft dileptons. In a thermal medium, however, $\pi^+\pi^-\rightarrow e^+e^-$ is not the only process which has to be considered. For example, the contribution from the two-body reaction $\pi^+\pi^-\rightarrow\rho\gamma^*\rightarrow\rho e^+e^-$ does not have a kinematical threshold at $2m_\pi$ and, therefore, certainly dominates the basic pion annihilation process for dilepton masses $M\simeq 2m_\pi$. This example indicates that a more complete analysis of the low mass dilepton spectrum originating from a possible thermal medium requires further considerations.

Previous calculations of the thermal rate of emission of direct, i.e., real, photons with energies less than 1 GeV have shown that there are two contributing reactions involving a neutral ρ: the annihilation process $\pi^+\pi^-\rightarrow\rho^0\gamma$ and Compton-like scattering $\pi^\pm\rho^0\rightarrow\pi^\pm\gamma$ [14]. Both contribute to dilepton production, where the real photon is replaced by a virtual one. The importance of two-body processes for low mass dileptons has also been stressed in the case of production from the quark-gluon plasma [15].

In this paper we compute the contributions to the dilepton production rate from π-ρ interactions for invariant masses up to the ρ peak. In Sec. II, after briefly treating the $\pi^+\pi^-\rightarrow\gamma^*$ Born rate, we discuss the ''real'' $2\rightarrow 2$ and $\rho\rightarrow\pi\pi\gamma^*$ reactions, at the two-loop level of the virtual photon self-energy. Also the ''virtual'' two-loop corrections to the Born rate are derived. Section III extends the estimates of

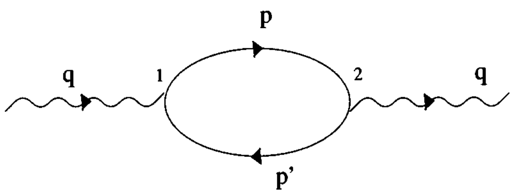

FIG. 1. One-loop photon self-energy diagram. The solid line denotes the pion.

the dilepton rate, taking into account out-of-equilibrium effects by introducing the pion chemical potential. Finally, in Sec. IV we compare the dilepton rate with experimental data [5] in the low mass region.

II. DILEPTON PRODUCTION AND π-ρ INTERACTIONS

The thermal dilepton production rate is considered in lowest order of the electromagnetic coupling. First, the medium is taken at rest. The rate per unit space-time volume, $dR \equiv dN/d^4x$, is related to the absorptive part of the photon self-energy tensor $\Pi_{\mu\nu}$ [2,11,16,17]. For lepton pairs of invariant mass M, energy q_0, and momentum $\vec{q}$ the relation is

$$\frac{dR}{dM^2 d^3q/q_0} = -\frac{\alpha}{24\pi^4 M^2} n(q_0) \mathrm{Im}\Pi^{\mu}{}_{\mu}(q_0,\vec{q}), \qquad (1)$$

where n is the Bose distribution function at temperature $T=1/\beta$ (cf. Appendix A). The tensor is constrained by current conservation $q_\nu \Pi^{\nu}{}_{\mu}(q)=0$.

We adopt the real-time formulation of finite temperature field theory to evaluate $\mathrm{Im}\Pi^{\mu}_{\mu}$. Using the Keldysh variant (with time path parameter $\sigma=0$ [18–20]) the following useful relation holds in terms of the photon–self-energy matrix Π^{γ}_{ab}:

$$\mathrm{Im}\Pi^{\mu}{}_{\mu}(q_0,\vec{q}) = \frac{1}{2n(q_0)} i\Pi^{\gamma}_{12}(q_0,\vec{q}). \qquad (2)$$

A. Born rate

In order to clarify the notation we give the one-loop expression for Π^{γ}_{12}. With the momentum labels indicated in Fig. 1 this pion-loop contribution with the temperature-dependent propagators (A1), summarized in Appendix A, reads

$$i\Pi^{\gamma}_{12}(q_0,\vec{q}) = -(-ie)^2 \int \frac{d^4p}{(2\pi)^4}(p+p')^2 iD_{12}(p) iD_{21}(p'), \qquad (3)$$

where $p'=p-q$.

Using the equilibrium distributions one recovers the standard expression for the Born term $\pi^+\pi^- \to \gamma^* \to l^+ l^-$. For masses M near the ρ it is appropriate [11] to implement the vector dominance model (VDM) and to insert the pion electromagnetic form factor F_π,

$$|F_\pi(M)|^2 = \frac{m_\rho^4}{(M^2-m_\rho^{*2})^2+\Gamma_\rho^2 m_\rho^2}, \qquad (4)$$

into the production rate. For our numerical analysis the parameters are chosen as $m_\rho = 0.775$ GeV, $m_\rho^* = 0.761$ GeV, and $\Gamma_\rho = 0.118$ GeV, in agreement with the measured pion electromagnetic form factor [11]. We do not consider the possibility of medium-dependent resonance parameters, as done in [7]. Also contributions due to the $A1$ resonance [21] are neglected.

For soft dileptons with invariant masses $M < m_\rho$ the mass distribution per unit space-time volume is obtained within a very good approximation from the rate with the heavy photon taken at rest with respect to the medium (also kept at rest) [3,10],

$$\frac{dN}{dM^2 d^4x} \simeq 4\pi T^2 \left(\frac{\pi M}{2T}\right)^{1/2} \left.\frac{dR}{dM^2 d^3q/q_0}\right|_{\vec{q}=0}, \qquad (5)$$

where the Born rate for $M \simeq m_\rho$, with the Boltzmann approximation of the pion distribution, has the simple form

$$\left.\frac{dR^{\mathrm{Born}}}{dM^2 d^3q/q_0}\right|_{\vec{q}=0} = \frac{\alpha^2}{96\pi^4} |F_\pi(M)|^2 \exp(-M/T). \qquad (6)$$

The more complete expression for the Born contribution with quantum statistics and arbitrary heavy photon momentum is, however, also well known in the literature (see, e.g., [4]). It will be used in the following numerical estimates. Throughout the paper we neglect the pion mass (except for the numerical analysis of the Born rate for $M < m_\rho$) and the masses of the leptons. Because of the many uncertainties, we believe that these approximations are very well justified.

Taking into account out-of-equilibrium effects in determining the rates, expression (6) is multiplied by a factor

$$1 + 2\delta\lambda, \qquad (7)$$

with $\delta\lambda = \lambda - 1$ in terms of the fugacity λ (cf. Appendix A). This first approximation, i.e., staying near equilibrium for $\delta\lambda \ll 1$ and neglecting more complicated dependences, should indicate the possible increase ($\lambda > 1$) or the decrease ($\lambda < 1$) of the dilepton rate due to nonequilibrium effects.

B. Two-loop contributions

The interaction of the charged pions with the neutral massive rho meson field ρ_μ and the electromagnetic potential A_μ is described by the Lagrangian [14]

$$L = |D_\mu \Phi|^2 - \tfrac{1}{4}\rho_{\mu\nu}\rho^{\mu\nu} + \tfrac{1}{2} m_\rho^2 \rho_\nu \rho^\nu - \tfrac{1}{4} F_{\mu\nu}F^{\mu\nu}, \qquad (8)$$

where $D_\mu \equiv \partial_\mu - ieA_\mu - ig_\rho \rho_\mu$ is the covariant derivative, Φ is the complex pion field, $\rho_{\mu\nu}$ is the rho, and $F_{\mu\nu}$ is the photon field strength tensor. As is well known, the $\rho\pi\pi$ coupling is rather large $g_\rho^2/4\pi \simeq 2.9$; nevertheless, we attempt an effective perturbative treatment up to two loops. However, no resummation of high temperature effects, e.g., comparable to the hard thermal loop expansion for QCD [22,23], is implemented in our approach, which may be compared with an analogous fixed-order calculation for dilepton production from a quark-gluon plasma [24].

From the Lagrangian (8) and using the closed-time-path formalism [18,19] we calculate the dilepton production rate produced in a thermal pionic medium at the two-level level.

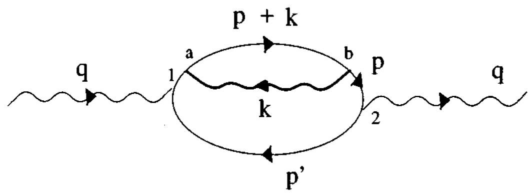

FIG. 2. Two-loop diagram: self-energy insertion. The labels a,b $=1,2$ denote the type of $\pi\rho$ vertex. The solid line with momentum label k corresponds to the ρ.

Typical diagrams are shown in Figs. 2 and 3. The two tadpole diagrams of $O(g_\rho^2)$ are not included, since they do not contribute to the discontinuity of the photon self-energy (2).

1. Real ρ^0 processes

The processes involving real ρ^0's, namely, $\pi\pi\to\rho\gamma^*$, $\pi\rho\to\pi\gamma^*$, and $\rho\to\pi\pi\gamma^*$, are expected to be important for dilepton masses M below the ρ peak. These contributions are obtained by cutting the two-loop diagrams (Figs. 2 and 3) such that the ρ is put on mass shell.

We start to discuss explicitly the contribution from the diagram shown in Fig. 2, where the self-energy correction $\delta D_{12}(p)$ is inserted into the pion line with momentum p. The expression for $\delta D_{12}(p)$ is derived in Appendix B using the Dyson equation.

In this section we assume (thermal and chemical) equilibrium distributions (A3), and consequently we use $\delta D_{12}^{\rm eq}(p)$ given in Eq. (B5). The discussion of out-off-equilibrium effects in the γ^* rate is postponed to Sec. III.

Using the second term of Eq. (B5) we calculate the ''real'' correction to Eq. (3):

$$i\delta\Pi_{12}^{\gamma,SE}(q^0,\vec{q})=-(-ie)^2\int\frac{d^4p}{(2\pi)^4}(p+p')^2\mathbf{P}\left(\frac{1}{p^2}\right)^2 \times[-i\Pi_{12}(p)]iD_{21}(p'), \tag{9}$$

where the pion self-energy $i\Pi_{12}(p)$ at one-loop order due to $\pi\rho$ interactions (8) is given by [cf. Eqs. (B6) and (C2)]

$$i\Pi_{12}(p)=g_\rho^2\int\frac{d^4k}{(2\pi)^4}(2p+k)^\sigma\left(-g_{\sigma\tau}+\frac{k_\sigma k_\tau}{m_\rho^2}\right) \times(2p+k)^\tau D_{12}(p+k)D_{21}(k). \tag{10}$$

We note that in Eq. (9) we only keep the real ρ^0 contributions.

Inserting the propagators (A1) with Eq. (A9) it is convenient to separate the different kinematical configurations, which appear due to the presence of the sign function in Eq. (A9). We consider in more detail the process of ρ emission, i.e., $\pi(p_+)+\pi(p_-)\to\rho(k)+\gamma^*(q)$, where we relabel the momenta of Fig. 2 as $p'\to -p_-,p\to p_+-k$, and introduce (positive) energies $k^0=E_\rho, p_-^0=E_-, p_+^0=E_+$. We find the following contribution to $i\delta\Pi_{12}^{\rm SE}$ of Eq. (9):

$$+\,4e^2g_\rho^2\int\frac{d^3p_+}{(2\pi)^3 2E_+}n(E_+)\int\frac{d^3p_-}{(2\pi)^3 2E_-}n(E_-) \times\int\frac{d^3k}{(2\pi)^3 2E_\rho}[1+n(E_\rho)](2\pi)^4\delta^4(p_++p_--k-q) \times(2p_--q)^2\mathbf{P}\left(\frac{1}{(p_+-k)^2}\right)^2 p_+^\sigma\left(-g_{\sigma\tau}+\frac{k_\sigma k_\tau}{m_\rho^2}\right)p_+^\tau, \tag{11}$$

expressed in a form familiar from kinetic theory [2]: It consists of the square of the matrix element for the two-body process $\pi\pi\to\rho\gamma^*$, here to one of the exchange diagrams plotted in Fig. 4, with the integration over the phase space of the participating pions and the ρ meson properly weighted by the thermal distribution functions $n(E)$. Next we also integrate with respect to the photon momentum $\vec{q}$ as described in Appendix D.

An analogous, straightforward treatment gives the corresponding contributions to the real ρ^0 processes from the two-loop vertex type diagrams of Fig. 3. Finally we sum all these

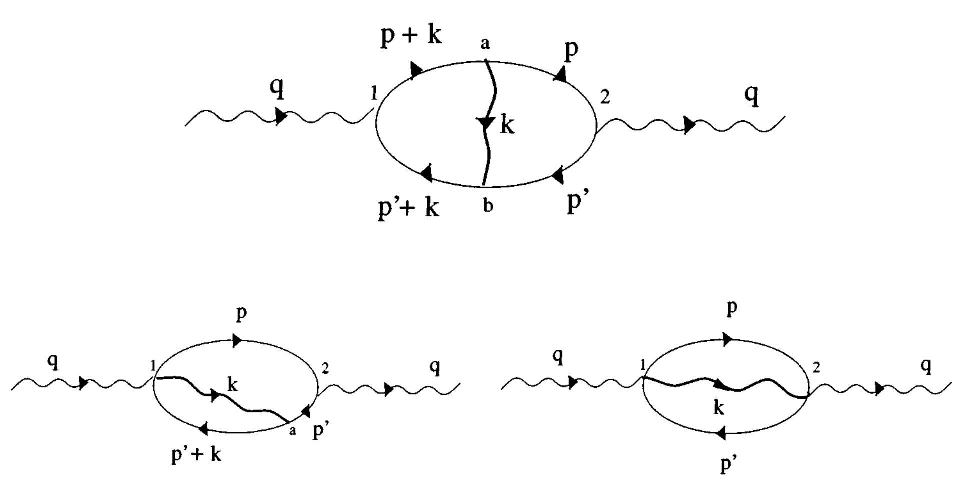

FIG. 3. Two-loop diagrams: vertex-type corrections.

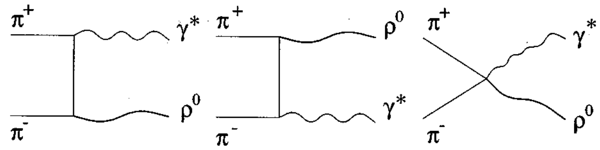

FIG. 4. Matrix elements for the process $\pi\pi\rightarrow\rho\gamma^*$ arising from cutting the two-loop diagrams.

contributions, including those obtained by interchanging momenta, like the self-energy contribution of Eq. (9), but interchanging p and p' in Fig. 2.

As a check the same final result is obtained when the square of the sum of the three matrix elements illustrated in Fig. 4 is taken. This approach has, e.g., the advantage that current conservation is rather easily checked on the level of these matrix elements.

Here we quote the result. Mainly for simplicity we use the Boltzmann approximation which amounts to underestimating the dilepton rate: In this limit we replace, e.g., in Eq. (11), $n(E_+)n(E_-)\rightarrow\exp(-E_+-E_-)/T$, and neglect stimulated emission, $1+n(E_\rho)\simeq 1$. The dilepton rate due to the real ρ^0 processes is best expressed using the Mandelstam variables defined in Eq. (D4); together with the kinematical approximations discussed in Appendix D, we obtain, for the dilepton mass range $M\leqslant m_\rho$,

$$\frac{dN^{\text{real}}}{dM^2d^4x}\simeq\frac{\alpha^2g_\rho^2/4\pi}{24\pi^4M^2}\sqrt{\frac{\pi T^3}{2m_\rho^3}}\Bigg\{\Bigg[\int_{(m_\rho+M)^2}^{\infty}ds\exp\left(-\frac{s+m_\rho^2-M^2}{2m_\rho T}\right)+\int_0^{(m_\rho-M)^2}ds\,e^{-m_\rho/T}\Bigg]\int_{u_-}^{u_+}du$$
$$+2\,\mathbf{P}\int_{m_\rho^2}^{\infty}dt\exp\left(-\frac{t+m_\rho^2}{2m_\rho T}\right)\int_{u_{\min}}^{u_{\max}}du\Bigg\}\left[2+\frac{m_\rho^2M^2}{4}\left(\frac{1}{t^2}+\frac{1}{u^2}\right)+\frac{(m_\rho^2+M^2)^2+m_\rho^2M^2/2}{tu}-(m_\rho^2+M^2)\left(\frac{1}{t}+\frac{1}{u}\right)\right],\quad(12)$$

where

$$u_{\substack{+\\(-)}}=\frac{1}{2}(m_\rho^2+M^2-s)\,\substack{+\\(-)}\,\frac{1}{2}\sqrt{[s-(m_\rho+M)^2][s-(m_\rho-M)^2]},\quad u_{\max}=m_\rho^2M^2/t,\quad u_{\min}=m_\rho^2+M^2-t,\qquad(13)$$

with $s+t+u=m_\rho^2+M^2$. The u integration may still be performed analytically.

The kinematic boundaries of integration given for the processes, which are summed in Eq. (12) in the order of $\pi\pi\rightarrow\rho\gamma^*$, $\rho\rightarrow\pi\pi\gamma^*$, $\pi\rho\rightarrow\pi\gamma^*$, are illustrated in the Mandelstam plot of Fig. 8.

The result contained in Eq. (12), for the squared matrix elements of Fig. 4, is sucessfully compared with the one derived in [14] for the case of the two-body processes involving a real photon.

It is important to note that due to the nonvanishing ρ mass and the heavy photon, $M>0$, no mass singularities appear in Eq. (12), even when setting the $T=0$ pion mass to zero. However, for the evaluation of the $\pi\rho\rightarrow\pi\gamma^*$ contribution, the principial value prescription leading to a well-defined integral, e.g., in Eq. (12), $\mathbf{P}(1/u)\equiv\lim_{\varepsilon\rightarrow 0}u/(u^2+\varepsilon^2)$, and correspondingly for $\mathbf{P}(1/u^2)$ [18], has to be taken into account, in order to correctly treat the behavior near $u\simeq 0$, which is covered by the kinematical domain of this process (Fig. 8). For the processes $\pi\pi\rightarrow\rho\gamma^*$ and $\rho\rightarrow\pi\pi\gamma^*$ the $\mathbf{P}$ prescription is not explicitly required.

We plot the rate Eq. (12) below the ρ peak in Fig. 5 as a function of the dilepton mass M for $M\geqslant 0.2$ GeV at fixed temperature $T=150$ MeV. For comparison the Born rate $\pi\pi\rightarrow\gamma^*$ is also included. We find that, as expected, the two-body reactions $\pi\pi\rightarrow\rho\gamma^*$ and $\pi\rho\rightarrow\pi\gamma^*$, together with the decay channel $\rho\rightarrow\pi\pi\gamma^*$, dominate the dilepton rate for low masses.[1] Thus, when discussing the thermal yield in the context of recent experimental data on dilepton production in heavy ion collisions, it is necessary to include the above higher order processes.

It is worth to mention that admitting in-medium effects on the ρ meson mass or width, as recently proposed in Refs. [7, 9, 10], could substantially influence the overall thermal rate (solid curve) shown in Fig. 5. In particular, assuming a decrease of the ρ meson mass by only 100 MeV would imply an increase of the thermal rate (solid curve of Fig. 5) by a factor of 2.

2. *Virtual ρ^0 processes*

For heavy photon production at $O(g_\rho^2)$ we have, in order to correct the Born rate (6), to include virtual contributions, which arise from the processes shown in Figs. 2 and 3 by cutting the diagrams in the proper way only through pion lines, without cutting the ρ line. For the production of real photons [14] these contributions are absent.

In some detail we describe our estimate, including the approximations, for the self-energy diagram (Fig. 2). Here

[1]We note that the curves do not strongly change when the kinematical approximations performed in Appendix D are relaxed, e.g., for $\pi\pi\rightarrow\rho\gamma^*$ at most a 10% change is numerically found when the ρ is not kinematically kept fixed at rest.

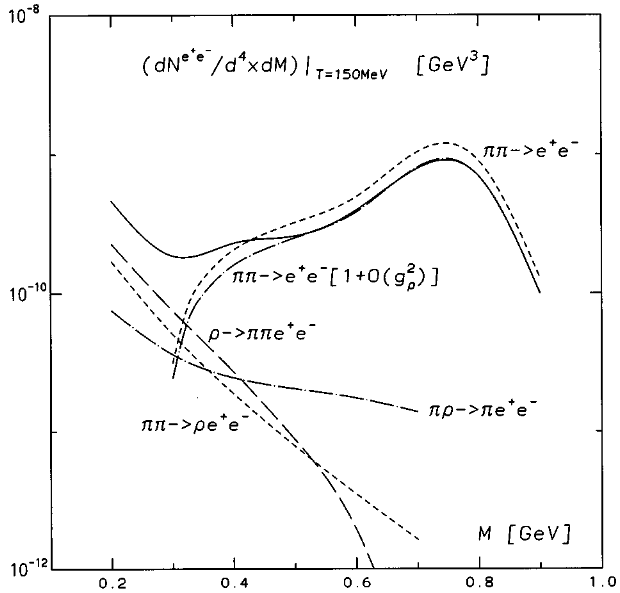

FIG. 5. Dilepton rate as a function of M at fixed $T=150$ MeV. The solid curve represents the sum of the real and the virtual processes.

we take the first term of Eq. (B5) and evaluate [cf. Eq. (9)]

$$i\delta\Pi_{12}^{\gamma,\mathrm{virt\,SE}}(q^0,\vec{q})=(-ie)^2\int\frac{d^4p'}{(2\pi)^3}(p+p')^2 \times\epsilon(p_0)n(p_0)\delta'(p^2) \times\mathrm{Re}\Pi(p)iD_{21}(p'), \tag{14}$$

where now the real part of the pion self-energy $\Pi(p)$ enters, and equilibrium distributions are used.

In the following the on-shell behavior of the pion self-energy, ReΠ, at the one-loop level is required. According to [13] its temperature-independent part is absorbed into the definition of the $T=0$ pion mass (which we take approximately as $m_\pi=0$). Its temperature-dependent part is weighted by the thermal distribution either for the ρ meson or for the pion. The first case is of $O(\exp(-m_\rho/T))$, i.e., negligible; the second one therefore dominates and is expected to be of $O(T^2/m_\rho^2)$, due to the presence of the $T=0$ $\rho-$propagator in the loop (Fig. 2).

In the following we estimate Eq. (14) in the limit $m_\rho \gg T$, having in mind the mass region $M\leqslant m_\rho$. To obtain the result analytically we make the further simplifying assumption of dileptons at rest [cf. Eq. (5)]. Then it is straightforward to find

$$i\delta\Pi_{12}^{\gamma,\mathrm{virt\,SE}}(M,\vec{q}=0)=e^2\int\frac{d^3p'}{(2\pi)^2}\frac{1}{2E'}n(E')n(M-E') \times\delta'(M/2-E')(E'/M-1/4) \times\mathrm{Re}\Pi(M-E',-\vec{p'}), \tag{15}$$

where $|\vec{p'}|=E'$.

When evaluating Re$\Pi(p_0,\vec{p})$ on shell, we get

$$\mathrm{Re}\Pi(M/2,\vec{p})\simeq O(M^2(T/m_\rho)^4), \tag{16}$$

for $|\vec{p}|=M/2$, and therefore it will be neglected. The leading term of Eq. (15) is found after partial integration with respect to the variable E'; it is proportional to the derivative

$$\frac{\partial}{\partial E'}\mathrm{Re}\Pi\simeq-\frac{g_\rho^2}{4\pi^2}M\frac{T^2}{m_\rho^2}, \tag{17}$$

when evaluated on shell because of the δ-function constraint in Eq. (15), and using Boltzmann distributions. As expected we obtain

$$i\delta\Pi_{12}^{\gamma,\mathrm{virt\,SE}}(M,\vec{q}=0)\simeq-\frac{e^2}{8\pi^2}\frac{g_\rho^2}{4\pi}M^2\frac{T^2}{m_\rho^2}\exp(-M/T), \tag{18}$$

where we already include a factor of 2 for the diagram Fig. 2 after interchanging p with p'.

In an analogous treatment we evaluate the virtual T-dependent contributions from the vertex-type diagrams, namely, from the first two of Fig. 3. After a lengthy calculation the result is

$$\frac{dN^{\mathrm{Born+virtual}}}{dM^2d^4x}\simeq\frac{dN^{\mathrm{Born}}}{dM^2d^4x}\left[1+\frac{g_\rho^2}{4\pi}\left(\frac{T}{m_\rho}\right)^2\left(-\frac{19}{3\pi}+\frac{M^2}{6\pi T^2}\mathbf{P}\int_0^\infty n(k)\frac{kdk}{(k^2-M^2/4)}\right)\right] \simeq\frac{dN^{\mathrm{Born}}}{dM^2d^4x}\left[1-\frac{7}{\pi}\frac{g_\rho^2}{4\pi}\left(\frac{T}{m_\rho}\right)^2\right], \tag{19}$$

valid for $m_\rho \gg T$, and for $M>0$.

In Fig. 5 we see that, e.g., for $T=150$ MeV, the T-dependent virtual corrections (19) are negative and rather large. It suggests to perform resummations, which, however, we do not attempt.

III. OUT-OF-EQUILIBRIUM EFFECTS

In the early stage of heavy ion collisions, when lepton pairs are expected to be predominantly produced [1–4], it is more likely that the pion gas is not yet in thermal and chemical equilibrium [25,26]. Before we treat the realistic situation of an expanding gas in the next section, we first have to compute the production rate using nonequilibrium distributions, thus generalizing the calculation of Sec. II. We proceed with a tractable, but still realistic ansatz [25,26] by introducing the fugacity parameter [27] λ and by using the distributions[2] $\tilde{n}(|k_0|)\simeq\lambda e^{-|k_0|/T}$ in Boltzmann approximation [cf. Eqs. (A6) and (A7)]. We have in mind that $\delta\lambda\equiv\lambda-1$ is small $\delta\lambda\ll1$, i.e., a situation not far off equilibrium, in order to be consistent with the simplifying approximations summarized in Appendix A.

In order to estimate nonequilibrium effects even under these approximations it is not justified to simply multiply the

[2]We do not distinguish the fugacity parameter for $\pi^\pm$ and ρ, respectively.

real emission rate (12) by a factor $(1+2\delta\lambda)$ as it is in the case of the Born rate [cf. Eq. (7)]. Because of the structure of the (one-loop) self-energy correction to the pion propagator (B3), a more careful derivation is required. For the real emission contribution it first amounts to the replacement of Eq. (9) by

$$i\delta\Pi_{12}^{\gamma,\mathrm{off}}(q^0,\vec{q})\simeq-(-ie)^2\int\frac{d^4p}{(2\pi)^4}(p+p')^2 \times\Biggl\{\mathbf{P}\left(\frac{1}{p^2}\right)^2 n(p_0)[i\Pi_{12}(p)-i\Pi_{21}(p)] +\frac{1}{(p^2)^2+(p_0\gamma)^2}\{n(p_0)i\Pi_{21}(p) -[1+n(p_0)]i\Pi_{12}(p)\}\Biggr\}iD_{21}(p'), \quad (20)$$

where again a corresponding term with $(p\leftrightarrow p')$ has to be added. In the second term in Eq. (20) the pinch singularity, which is not canceled in case of nonequilibrium distributions [28], is regularized [29] by the damping rate γ of the pion, which we estimate in Appendix C. The expression for $i\Pi_{12}(p)$ is the same as in Eq. (10), except that it now has to be evaluated using the nonequilibrium distributions (A6), as it is the case for $n(p_0)$ in Eq. (20).

We here discuss further details of the estimate for the dominant contribution, which is due to $\pi\rho\to\pi\gamma^\star$ in the limit $\gamma\to0$, in order to exhibit our treatment, i.e., the regularization of the pinch singularities in the vincinity of $t/u\simeq0$ (cf. Fig. 8).

It is crucial to consider the product of distributions, which is present in Eq. (20),

$$[1+n(p_0')]\{n(p_0)n(k_0)[1+n(p_0+k_0)] -[1+n(p_0)][1+n(k_0)]n(p_0+k_0)\}, \quad (21)$$

adjusted for the kinematics of the process $\pi(p_{\mathrm{in}})+\rho(k_\rho)\to\pi(p_{\mathrm{out}})+\gamma(q)$, i.e., $p'\to-p_{\mathrm{in}}$, $k\to-k_\rho$, $p\to-p_{\mathrm{out}}+k_\rho$ (cf. Fig. 2). In relation to the definitions (D4) we have to continue: $k\to-k_\rho$, $p_+\to-p_{\mathrm{out}}$, $p_-\to p_{\mathrm{in}}$, which corresponds to the physical region (ii) with $u\geqslant m_\rho^2$ in Fig. 8. The limit $\gamma\to0$ is sensitive to the behavior near $t=(k_\rho-p_{\mathrm{out}})^2\simeq0$. In the simplifying kinematical approximation of the ρ meson at rest, $E_\rho\simeq m_\rho$, used in Appendix D, the region $t\simeq0$ corresponds to positive energy $p_0\simeq(t+m_\rho^2)/2m_\rho>0$.

Thus the product of distributions (21) reads, in the Boltzmann approximation,

$$-\lambda^2(\lambda-1)e^{(E_\rho+E_{\mathrm{out}})/T}\simeq-\delta\lambda e^{-(u+m_\rho^2)/2m_\rho T}, \quad (22)$$

valid for $p_0>0$ and in leading order of $\delta\lambda$. The dominant contribution arising from Eq. (20) to the dilepton spectrum becomes

$$\frac{dN^{\mathrm{pinch}}}{dM^2d^4x}\overset{\gamma\to0}{\simeq}-\delta\lambda\frac{\alpha^2(g_\rho^2/4\pi)}{48\pi^4M^2}\sqrt{\frac{\pi T^3}{2m_\rho^3}} \times\left\{\int_{m_\rho^2}^{2m_\rho^2+M^2}du\,e^{-(u+m_\rho^2)/2m_\rho T}\int_{t_{\mathrm{min}}}^{t_{\mathrm{max}}}dt +\int_{2m_\rho^2+M^2}^{\infty}du\,e^{-(u+m_\rho^2)/2m_\rho T}\int_{-m_\rho^2}^{t_{\mathrm{max}}}dt\right\} \times\frac{m_\rho^2M^2}{t^2+[g_\rho^2T^2/4\pi e]^2}, \quad (23)$$

where we take into account by a factor of 2 both regions denoted by (ii) in Fig. 8. The boundaries of the integrations are defined as in Eq. (13), except for $t\leftrightarrow u$. When using in Eq. (23) the momentum-independent value for the damping γ, Eq. (C5), the integrations can be explicitly performed. The leading term with $\gamma\to0$ is proportional to $1/\gamma$, indicating the pinch singularity,

$$\frac{dN^{\mathrm{pinch}}}{dM^2d^4x}\simeq-\delta\lambda\frac{\alpha^2(g_\rho^2/4\pi)}{24\pi^3} \times\sqrt{\frac{\pi T^3}{2m_\rho^3}}\frac{m_\rho^3}{g_\rho^2/(4\pi e)T}e^{-(2m_\rho^2+M^2)/2m_\rho T}, \quad (24)$$

which is actually independent of the coupling g_ρ^2. From Fig. 8 one can read off that the pinch near $t\simeq0$ is present starting at $u\geqslant m_\rho^2+M^2$. This and Eq. (22) explain the argument of the exponential function in Eq. (24).

We remark that Eq. (24) differs numerically by only a few percent from the more exact expression starting from Eq. (20) and including all the contributions due to the processes (i)–(iii) defined in Appendix D.

In Fig. 6 we plot the total rate dN/dMd^4x, including the Born term with $O(g_\rho^2)$ correction, for nonequilibrium cases characterized by different values of the chemical potential μ, including even as large values as $\mu=100$ MeV, which corresponds to a large value of $\lambda\simeq1.95$ at $T=150$ MeV. Although here $\delta\lambda$ may be considered too large to justify keeping only $O(\delta\lambda)$ terms,[3] as done in the calculation of the curves plotted in Fig. 6, we observe that instead of an expected increase by a factor of $\lambda^2\simeq4$, only an effective increase of the rate by a factor of 2 results, because of the negative contribution estimated in Eq. (24), when we change μ from $\mu=0$ to $\mu=100$ MeV. From this fact we stress the importance of taking into account the nontrivial term (20), which is traced back to the self-energy diagram (Fig. 2). For completeness we state that no such extra terms arise from the vertex type diagrams of Fig. 3.

IV. SOFT DILEPTONS IN THE EXPANDING HADRONIC MEDIUM

In the previous sections we have derived the dilepton production rate originating from π-ρ interactions up to

[3]A different estimate in case of large λ, namely, replacing $\gamma\to\lambda\gamma$, and Born$(1+O(g_\rho^2))\to\lambda^2$Born$/[1-O(\lambda g_\rho^2)]$, etc., actually gives the same result as in Fig. 6.

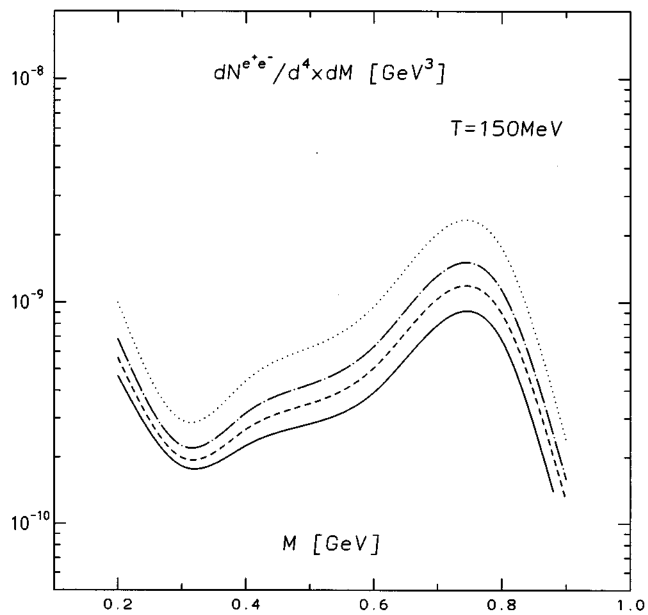

FIG. 6. Estimates of out of equilibrium effects to the dilepton rate up to $O(g_\rho^2)$ at fixed $T=150$ MeV: The solid curve corresponds to $\mu=0$, dashed curve to $\mu=25$, dash-dotted curve to $\mu=50$, and dotted curve to $\mu=100$ MeV, respectively.

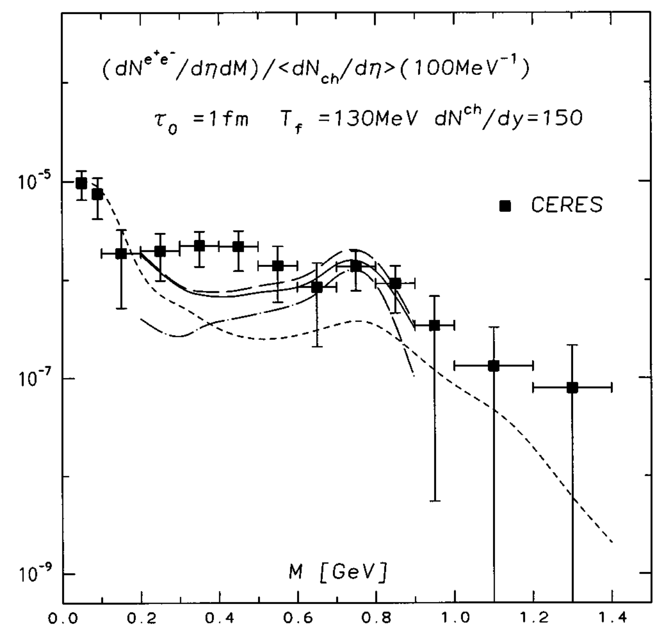

FIG. 7. Invariant-mass dielectron spectra measured by the CERES Collaboration for the S-Au collisions [5] in comparison with the thermal yield from π-ρ interactions. The dashed-dotted line describes the sum of all contributing reactions from $\pi^\pm$-ρ^0 interactions. The dashed line, calculated by CERES, represents the expected dielectron yield from all known hadronic sources. The solid line is the sum of the contributions described by the dash-dotted and dashed curves. The long-dashed curve includes the out-of-equilibrium effects.

$O(g_\rho^2)$ in a thermal medium as a function of temperature and for fixed chemical potential. In the description of dilepton spectra in heavy ion collisions we have in addition to take into account that dilepton pairs are emitted from a rapidly expanding and thereby cooling medium. Hot hadronic matter produced in heavy ion collisions undergoes an expansion, which leads to a space-time dependence of the thermal parameters. In the expanding system we therefore have to integrate the rates derived in the previous sections over the space-time history of the collision. As a model for the expansion dynamics we assume the Bjorken model for $(1+1)$-dimensional longitudinal hydrodynamical expansion [30]. In this model all thermodynamical parameters are only a function of the proper time τ and do not depend on the rapidity variable y. We furthermore assume that at some initial time $\tau_0\sim 1$ fm matter is formed as a thermalized hadronic gas with initial temperature T_0. The system subsequently expands and cools until it reaches the freeze-out temperature of $T_f\sim 130$ MeV. We have modeled the hadronic gas equation of state with a resonance gas where all hadrons and resonance states with masses up to 2.5 GeV are included. The value of the initial temperature $T_0\simeq 210$ MeV has been fixed by the requirement to reproduce the multiplicity of 150 charged pions in the final state at central rapidity. These numbers are for S-Au collisions [5].

With the above defined model for the expansion dynamics the space-time integration of the rates, first calculated in equilibrium, namely, the Born rate including the virtual correction of $O(g_\rho^2)$, Eq. (19), and the real processes, Eq. (12), can be performed leading to the spectrum which may than be compared with the one experimentally measured in heavy ion collisions. In Fig. 7 we show the overall thermal dilepton rate from π-ρ interactions including acceptance and kinematical cuts of the CERES experiment [5]. One can see in Fig. 7 that with the thermal source for dielectron pairs due to π-ρ interactions with the approximations as discussed in Sec. II one can partially account for the excess reported by the CERES Collaboration as measured in S-Au (and Pb-Au) collisions. This is particularly the case in the vicinity of the ρ peak where the agreement with the experimental data is quite satisfactory. However, the enhancement below the ρ peak and the structure of the distribution cannot be explained by equilibrium production alone. In the kinematical window $0.25<M<0.45$ GeV there are still almost 70% deviations of our theoretical curve from the experimental results. Assuming nonchemical equilibrium in the mesonic medium (as discussed in Sec. III) should certainly increase the dilepton rate. This is mostly because, in this case, there are more soft pions and ρ mesons, which should produce more abundant soft dileptons. In Fig. 7 we show the thermal rate (long-dashed curve) assuming deviations from chemical equilibrium with the value of the chemical potential $\mu=100$ MeV. Indeed, we observe an increase of the rate below the ρ peak. This increase, however, is rather modest, particularly in the soft part of the spectrum. The main reason is due to the ''pinch singular'' term (24), which being negative reduces the contributions of the two-loop processes, when considered out of equilibrium. In addition the out-of-equilibrium distributions of pions and ρ mesons lead to a lower initial temperature and a shorter lifetime of the thermal system. All these effects are the reason of small modifications of the dilepton yield.

Here, also additional assumptions, e.g., on in-medium effects of the ρ meson mass and width eventually help to understand more completely the dilepton excess measured by the CERES Collaboration [7,9,10].

V. SUMMARY

We have calculated the thermal production rate for soft dielectrons produced in a pion gas including relevant reactions from π-ρ interactions. The calculations include the $O(g_\rho^2)$ corrections arising from the two-loop contributions to the virtual photon self-energy. The dilepton rate is first calculated using equilibrium distributions. Next off-equilibrium contributions to the rates have been estimated. Finally, dilepton production in an expanding hadronic medium has been calculated applying the Bjorken model. No medium effects on the ρ resonance parameters are included in the analysis. The excess reported by the CERES Collaboration in the low mass range below the ρ peak is diminished, although not yet completely described by the model.

ACKNOWLEDGMENTS

One of us (K.R.) acknowledges stimulating discussion with members of the CERES Collaboration and partial support of the Gesellschaft für Schwerionenforschung (GSI) and of the Committee of Research Development Grant No. KBN 2-P03B-09908. This work was supported in part by the EEC Programme ''Human Capital and Mobility,'' Network ''Physics at High Energy Colliders,'' Contract No. CHRX-CT93-0357. M.D. was supported by Deutsche Forschungsgemeinschaft.

APPENDIX A: THERMAL PROPAGATORS

In order to perform the perturbative calculations presented in this paper we use the closed-time-path formalism of thermal field theory [18–20]. The real-time 2×2 matrix (scalar) propagators

$$\begin{aligned}
D_{11}(k) &= [1+n(k_0)]\Delta_R(k) - n(k_0)\Delta_A(k),\\
D_{12}(k) &= n(k_0)[\Delta_R(k)-\Delta_A(k)],\\
D_{21}(k) &= [1+n(k_0)][\Delta_R(k)-\Delta_A(k)],\\
D_{22}(k) &= n(k_0)\Delta_R(k) - [1+n(k_0)]\Delta_A(k)
\end{aligned} \tag{A1}$$

are expressed in terms of the retarded and advanced propagators

$$\Delta_{R(A)}(k) = \frac{1}{k^2 - m^2 \overset{+}{\underset{(-)}{}} i\epsilon k_0}, \tag{A2}$$

where $k^2 = k_0^2 - \vec{k}^2$ and m is the $T=0$ mass. For equilibrium conditions the Bose-Einstein distribution function $n(k_0)$ depends on temperature T,

$$n(k_0) = \frac{1}{e^{k_0/T}-1}, \tag{A3}$$

and satisfies

$$n(k_0) + n(-k_0) + 1 = 0. \tag{A4}$$

For our numerical estimates we are mainly using the Boltzmann approximation

$$n(|k_0|) \simeq \exp(-|k_0|/T). \tag{A5}$$

Estimating nonequilibrium effects we follow the approximations described in detail in [19] and, more recently, in [31]. It amounts to replacing the thermal $n(k_0)$, Eq. (A3), by their nonequilibrium counterparts, i.e., in general by Wigner distributions $n(k_0,X)$. This corresponds in terms of the cumulant expansion to approximate nonequilibrium correlations by the second cumulant only. As a further approximation we suppress the possible dependence on the center-of-mass coordinate X, essentially assuming a homogenous and isotropic medium.

Practically for our estimates we take [cf. Eq. (A4)]

$$n(k_0,X) \to \begin{cases} \tilde{n}(|k_0|), & k_0>0,\\ -(1+\tilde{n}(|k_0|), & k_0<0, \end{cases} \tag{A6}$$

with

$$\tilde{n}(|k_0|) \equiv \frac{1}{e^{(|k_0|-\mu)/T}-1} \hat{=} \frac{\lambda}{e^{|k_0|/T}-\lambda}, \tag{A7}$$

by introducing the fugacity parameter [27] $\lambda \equiv e^{\mu/T}$, which is assumed to be energy independent. Obviously $\lambda \neq 1$ in the case of (chemical) nonequilibrium. Consequently deviations from equilibrium are approximated in terms of the equilibrium distribution (A3) by

$$\frac{\delta n}{n(k_0)} \equiv n(k_0,X)/n(k_0) - 1 \simeq \delta\lambda\, \epsilon(k_0)[1+n(k_0)], \tag{A8}$$

in leading order of $\delta\lambda \equiv \lambda - 1$.

In the expressions for $\Delta_{R(A)}(k)$ the usual limit $\epsilon \to 0$ is considered, whenever this limit is defined, e.g.,

$$\Delta_R(k) - \Delta_A(k) = -2\pi i\, \epsilon(k_0)\, \delta(k^2-m^2), \tag{A9}$$

where $\epsilon(k_0) = \theta(k_0) - \theta(-k_0)$ is the sign function.

However, out-of-equilibrium pinch singularities appear in this limit $\epsilon \to 0$ [28], e.g., in products like $\Delta_R(k)\Delta_A(k)$ (see Appendix B). We treat this situation by following the conjecture by Altherr [29,32] keeping ϵ nonvanishing: It is identified by the damping width $\gamma > 0$ (Appendix C).

APPENDIX B: ONE-LOOP SELF-ENERGY CORRECTION TO THE PION PROPAGATOR

Here we comment (cf. Fig. 2) on the self-energy correction of the pion propagator and the possible appearence and presence of pinch singularities [18,28]. Denoting the self-energy insertion by the matrix $\Pi_{ab}(p)$ we obtain the improved D_{12} propagator using the Dyson equation

$$\begin{aligned}
iD_{12}(p) &\to iD_{12}(p) + \sum_{a,b=1,2} iD_{1a}(p)[-i\Pi_{ab}(p)]iD_{b2}(p)\\
&= iD_{12}(p) + i\,\delta D_{12}(p).
\end{aligned} \tag{B1}$$

With the propagators specified in Appendix A and with the relations

$$\Pi_{11}(p)=-\Pi^{\star}_{22}(p),\quad \mathrm{Im}\Pi_{11}=\frac{i}{2}(\Pi_{12}+\Pi_{21}),\quad \text{(B2)}$$

also valid out of equilibrium, we obtain

$$\delta D_{12}(p)=n(p_0)[\Delta_R^2(p)-\Delta_A^2(p)]\mathrm{Re}\Pi_{11}(p)+\frac{1}{2}n(p_0)\times[\Delta_R^2(p)+\Delta_A^2(p)][\Pi_{12}(p)-\Pi_{21}(p)]+\Delta_R(p)\Delta_A(p)\{n(p_0)\Pi_{21}(p)-[1+n(p_0)]\Pi_{12}(p)\}.\quad \text{(B3)}$$

Here the ill-defined product $\Delta_R(p)\Delta_A(p)$ appears, giving rise to possible unpleasant pinch singularities [18,28]. In case of equilibrium, however, it is well known that the last term in Eq. (B3) vanishes due to the detailed balance condition,

$$\Pi_{21}(p)=e^{p_0/T}\Pi_{12}(p).\quad \text{(B4)}$$

As a consequence Eq. (B3) simplifies to

$$\delta D_{12}^{\mathrm{eq}}(p)=2\pi i\epsilon(p_0)n(p_0)\left[\delta'(p^2)\mathrm{Re}\Pi(p)+\frac{1}{\pi}\mathbf{P}\left(\frac{1}{p^2}\right)^2\mathrm{Im}\Pi(p)\right],\quad \text{(B5)}$$

where

$$\mathrm{Re}\Pi(p)\equiv\mathrm{Re}\Pi_{11}(p),\quad \mathrm{Im}\Pi\equiv\frac{1}{2}\epsilon(p_0)\frac{i\Pi_{12}(p)}{n(p_0)},\quad \text{(B6)}$$

expressed in terms of the equilibrium distribution $n(p_0)$ and in terms of the (retarded) self-energy $\Pi(p_0+i\epsilon p_0,\vec{p})$ [23]. δ' denotes the derivative of the δ function and $\mathbf{P}$ the principal value.

However, for nonequilibrium distributions (A6), for which obviously $(1+n)/n\neq\exp(p_0/T)$, the last term in Eq. (B3) does not cancel. In order to regularize the product $\Delta_R(p)\Delta_A(p)$ [29] we take into account the nonvanishing (on-shell) damping rate of the pion, which we estimate in the following Appendix C.

APPENDIX C: ESTIMATE OF THE DAMPING RATE OF THE PION

The pion damping rate γ is determined by the ''pole'' (in the lower energy half-plane) of the retarded propagator. In the following we not only neglect the pion mass, but also thermal corrections due to the real part of the (retarded) pion self-energy, such that

$$\gamma\simeq-\frac{\mathrm{Im}\Pi(p_0,\vec{p})}{p_0},\quad \text{(C1)}$$

evaluated on shell $p^2=0$ for positive pion energy p_0. In the one-loop approximation the absorptive part of the pion self-energy is given by

$$\mathrm{Im}\Pi(p_0,\vec{p})=\frac{g_\rho^2}{2n(|p_0|)}\int\frac{d^4k}{(2\pi)^4}(2p+k)^\sigma\left(-g_{\sigma\tau}+\frac{k_\sigma k_\tau}{m_\rho^2}\right)\times(2p+k)^\tau D_{12}(p+k)D_{21}(k),\quad \text{(C2)}$$

where the momentum labels of Fig. 2 are used.

The temperature-dependent nonvanishing part for $p^2=p_0^2-\vec{p}^2=0$ becomes (cf. the derivation in [13])

$$\mathrm{Im}\Pi(p_0=p,|\vec{p}|=p)=-g_\rho^2m_\rho^2\pi\int\frac{d^3k}{(2\pi)^3}\frac{1}{2E_\rho 2E_\pi}[n(E_\pi)-n(E_\rho)]\delta(p-E_\rho+E_\pi),\quad \text{(C3)}$$

with the corresponding energies $E_\rho=\sqrt{\vec{k}^2+m_\rho^2}$ and $E_\pi=|\vec{p}+\vec{k}|$.

The dominant contribution comes from the pion's thermal distribution $n(E_\pi)$. In the Boltzmann approximation it leads to

$$\mathrm{Im}\Pi(p_0=p,p)\simeq-\frac{g_\rho^2}{4\pi}\frac{m_\rho^2}{4p}\int_{m_\rho^2/4p}^{\infty}n(E_\pi)dE_\pi\simeq-\frac{g_\rho^2}{4\pi}\frac{m_\rho^2T}{4p}e^{-m_\rho^2/4pT}.\quad \text{(C4)}$$

$\mathrm{Im}\Pi$ vanishes for $\vec{p}=0$, and it has its maximum near $p\simeq m_\rho^2/4T$. We note that Eq. (C4) gives a positive damping rate γ, as required. In order not to overestimate the contributions arising from the $\Delta_R\Delta_A$ terms we take for the numerical estimates a momentum-independent value, namely, the one at the maximum

$$p_0\gamma\simeq-\mathrm{Im}\Pi(p_0\simeq p,p)\simeq\frac{g_\rho^2}{4\pi}\frac{1}{e}T^2.\quad \text{(C5)}$$

APPENDIX D: KINEMATIC BOUNDARIES FOR THE KINETIC PROCESSES

The dilepton thermal rate receives contributions from the two-body processes $\pi\pi\to\rho\gamma^*$ and $\pi\rho\to\pi\gamma^*$, and from $\rho\to\pi\pi\gamma^*$, for which we evaluate in the following the phase-space integral (11) including its kinematic constraints. The calculation is simplified using (i) Boltzmann distributions and (ii) the fact that $m_\rho/T\gg1$: the ρ meson is kept at rest in the medium. This allows us to integrate the ρ's phase space by

$$I_\rho\hat{=}\int\frac{d^3k}{(2\pi)^3}\frac{1}{2E_\rho}e^{-E_\rho/T}\simeq\frac{T^2}{4\pi^2}\sqrt{\frac{\pi m_\rho}{2T}}e^{-m_\rho/T},\quad \text{(D1)}$$

and to replace elsewhere $E_\rho=\sqrt{\vec{k}^2+m_\rho^2}\simeq m_\rho$.

The remaining integrations are carried out as we explicitly show in the following for the channel $\pi(p_+)+\pi(p_-)\to\rho(k)+\gamma^*(q)$. We only consider the case of dilepton masses $M\leqslant m_\rho$.

The phase-space integral defined by

$$I \hat{=} \int \frac{d^3q}{q_0}\int \frac{d^3p_+}{(2\pi)^3 2E_+}\int \frac{d^3p_-}{(2\pi)^3 2E_-}\int \frac{d^3k}{(2\pi)^3 2E_\rho} \times e^{-E_\rho/T}(2\pi)^4\delta^4(p_+ + p_- - k - q) \quad \text{(D2)}$$

is approximated by

$$I \simeq \frac{1}{4\pi^2} I_\rho \int \frac{d^3p_+}{2E_+}\int \frac{d^3p_-}{2E_-}\frac{1}{q_0}\delta(E_+ + E_- - m_\rho - q_0), \quad \text{(D3)}$$

with $q_0 \simeq \sqrt{|\vec{p}_+ + \vec{p}_-|^2 + M^2}$. The angular integrations in I can be done.

Next we introduce the Mandelstam variables by

$$s = (p_+ + p_-)^2 = (k+q)^2, \quad t = (p_+ - k)^2 = (q - p_-)^2,$$
$$u = (p_- - k)^2 = (q - p_+)^2, \quad \text{(D4)}$$

with $s + t + u = m_\rho^2 + M^2$. Approximating the pion energies by

$$E_+ \simeq (m_\rho^2 - t)/2m_\rho, \quad E_- \simeq (m_\rho^2 - u)/2m_\rho \quad \text{(D5)}$$

gives the final result for the phase-space integral,

$$I \simeq \frac{1}{8m_\rho^2} I_\rho \int dt\,du\,\theta(tu - m_\rho^2 M^2)\,\theta(s - (m_\rho + M)^2). \quad \text{(D6)}$$

The other channels only differ in their kinematical boundaries,

$$\text{(ii)}\,\pi\rho \to \pi\gamma^*: \theta(-s)\,\theta(m_\rho^2 M^2 - tu), \quad \text{(D7)}$$

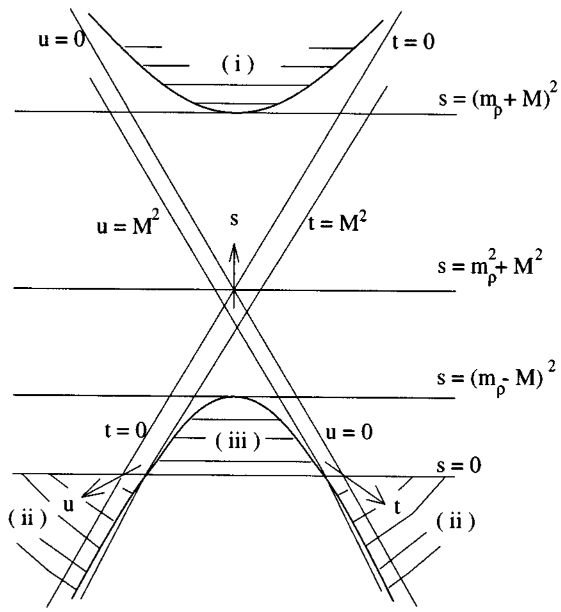

FIG. 8. Mandelstam plot: physical regions for the processes (i) $\pi\pi \to \rho\gamma^*$, (ii) $\pi\rho \to \pi\gamma^*$, and (iii) $\rho \to \pi\pi\gamma^*$.

$$\text{(iii)}\,\rho \to \pi\pi\gamma^*: \theta(s)\,\theta(tu - m_\rho^2 M^2),$$

which are also summarized in Fig. 8. The processes $\pi\pi\rho \to \gamma^*$ and $\pi \to \pi\rho\gamma^*$ do not contribute due to the nonvanishing masses m_ρ and M.

We finally remark that the poles at $t=0$ and/or $u=0$ are present within the kinematical domain for the channel $\pi\rho \to \pi\gamma^*$, whereas for $\pi\pi \to \rho\gamma^*$ they are present just at the kinematical boundary when $s \to \infty$.

[1] E. L. Feinberg, Nuovo Cimento A **34**, 391 (1976); E. Shuryak, Phys. Lett. **78B**, 150 (1978).
[2] L. McLerran and T. Toimela, Phys. Rev. D **31**, 545 (1985).
[3] P. V. Ruuskanen, in *Quark-Gluon Plasma*, edited by R. Hwa (World Scientific, Singapore, 1990); J. Alam, S. Raha, and B. Sinha, Phys. Rep. **273**, 243 (1996).
[4] J. Cleymans, K. Redlich, and H. Satz, Z. Phys. C **52**, 517 (1991).
[5] CERES Collaboration, G. Agakichiev *et al.*, Phys. Rev. Lett. **75**, 1272 (1995); P. Holl *et al.*, Report No. CERN-SPSLC-95-35 (unpublished).
[6] HELIOS/3 Collaboration, M. Masera, Nucl. Phys. **A590**, 3c (1995).
[7] G. Q. Li, C. M. Ko, and G. E. Brown, Phys. Rev. Lett. **75**, 4007 (1995); W. Cassing, W. Ehehalt, and C. M. Ko, Phys. Lett. B **363**, 35 (1995); V. Koch and C. Song, Phys. Rev. C **54**, 1903 (1996).
[8] D. K. Srivastava, B. Sinha, and C. Gale, Phys. Rev. C **53**, R567 (1996).
[9] C. Adami and G. E. Brown, Phys. Rep. **224**, 1 (1993); T. Hatsuda and S. H. Lee, Phys. Rev. C **46**, R34 (1992); G. Q. Li and C. M. Ko, Nucl. Phys. **A582**, 731 (1995); F. Karsch, K. Redlich, and L. Turko, Z. Phys. C **60**, 519 (1993); R. D. Pisarski, Phys. Rev. D **52**, R3773 (1995).
[10] C. Song, V. Koch, S. H. Lee, and C. M. Ko, Phys. Lett. B **366**, 379 (1996); G. Q. Li, C. M. Ko, and G. E. Brown, Nucl. Phys. **A606**, 568 (1996).
[11] C. Gale and J. I. Kapusta, Nucl. Phys. **B357**, 65 (1991); Phys. Rev. C **35**, 2107 (1987).
[12] C. Gale and P. Lichard, Phys. Rev. D **49**, 3338 (1994).
[13] C. Song, Phys. Lett. B **329**, 312 (1994); Phys. Rev. D **49**, 1556 (1994); **48**, 1375 (1993).
[14] J. I. Kapusta, P. Lichard, and D. Seibert, Phys. Rev. D **44**, 2774 (1991).
[15] E. Braaten, R. D. Pisarski, and T. C. Yuan, Phys. Rev. Lett. **64**, 2242 (1990); S. M. H. Wong, Z. Phys. C **53**, 465 (1992).
[16] H. A. Weldon, Phys. Rev. D **42**, 2384 (1990).
[17] H. A. Weldon, Phys. Rev. D **28**, 2007 (1983); R. L. Kobes and S. W. Semenoff, Nucl. Phys. **B260**, 714 (1985).
[18] N. P. Landsman and Ch. G. van Weert, Phys. Rep. **145**, 141 (1987).
[19] K.-C. Chou, Z.-B. Su, B.-L. Hao, and L. Yu, Phys. Rep. **118**, 1 (1985).
[20] M. A. van Eijck and Ch. G. van Weert, Phys. Lett. B **278**, 305 (1992).
[21] K. L. Haglin, Phys. Rev. C **53**, R2606 (1996); see also J. V.

Steele, H. Yamagishi, and I. Zahed, Phys. Lett. B **384**, 255 (1996); C. M. Hung and E. V. Shuryak, Report No. SUNY-NTG-96-16, hep-ph/9608299 (unpublished).

[22] R. D. Pisarski, Phys. Rev. Lett. **63**, 1129 (1989); E. Braaten and R. D. Pisarski, Nucl. Phys. **B337**, 569 (1990); R. D. Pisarski, Nucl. Phys. **A525**, 175c (1991), and references therein.

[23] M. Le Bellac, *Thermal Field Theory* (Cambridge University Press, Cambridge, England, 1996), and references therein.

[24] See, e.g., R. Baier, B. Pire, and D. Schiff, Phys. Rev. D **38**, 2814 (1988); T. Altherr and P. Aurenche, Z. Phys. C **45**, 99 (1989).

[25] S. Gavin, Nucl. Phys. **B351**, 561 (1991); S. Gavin and P. V. Ruuskanen, Phys. Lett. B **262**, 326 (1991).

[26] P. Koch, Z. Phys. C **57**, 283 (1993); B. Kämpfer, P. Koch, and O. P. Pavlenko, Phys. Rev. C **49**, 1132 (1994).

[27] S. R. de Groot, W. A. van Leeuwen, and Ch. G. van Weert, *Relativistic Kinetic Theory* (North-Holland, Amsterdam, 1980); see also T. S. Biro *et al.*, Phys. Rev. C **48**, 1275 (1993).

[28] T. Altherr and D. Seibert, Phys. Lett. B **333**, 149 (1994).

[29] T. Altherr, Phys. Lett. B **341**, 325 (1995).

[30] J. D. Bjorken, Phys. Rev. D **27**, 140 (1983).

[31] M. Le Bellac and H. Mabilat, Report No. INLN 96/17, 1996 (unpublished).

[32] For a discussion of pinch singularities, which differs from [29], see P. F. Bedaque, Phys. Lett. B **344**, 23 (1995).